Residual Generator Computation via Polynomial Approach for Fault Detection and Isolation in Dynamic Processes

M. Bonfè[1], *P. Castaldi*[2], *W. Geri* [2] *and S. Simani*[1]

[1] Dipartimento di Ingegneria. Università di Ferrara
Via Saragat 1, 44100 Ferrara, Italy. E-mail: sbeghelli@ing.unife.it
Ph: +39 0532 97 4830. Fax: +39 0532 97 4870

[2] Aerospace Engineering Faculty. University of Bologna
Via Fontanelle 40, 40136 Forlì, Italy

Abstract

This paper addresses the problem of the detection and isolation of the input and output sensor faults on a general aviation aircraft, characterised by a non–linear model, in the presence of wind gust disturbance and measurement errors. In particular, this work investigates the design of residual generators in order to realise complete diagnosis schemes when additive faults are present. The use of an input–output description for the linearised model of the aircraft allows to compute in a straightforward way the residual generators for fault detection and isolation. These tools lead to dynamic filters that can achieve both good disturbance signal de–coupling and robustness properties with respect to both linearisation error and measurement noise. Mathematical descriptions of the aircraft measurement sensors are also taken into account. The results obtained in the simulation of the faulty behaviour of a PIPER PA30 aircraft are finally reported.

Keywords: Fault detection and isolation, aerospace application, flight control, filter design, polynomial methods.

1 Introduction

There is a growing demand for higher reliability of aircraft and aerospace systems. Sensors are the most important components for flight control and aircraft safety and, as they work in a harsh environment, fault probabilities are high thus making these devices the least reliable components of the system.

In order to improve the reliability of the system sensors hardware and software (analytical) redundancy schemes have been investigated over the last twenty years [1, 2, 3, 4, 5, 6, 7, 8, 9, 10, 11].

Traditional approaches to fault detection in the wider application context are based on hardware redundancy methods which use multiple lanes of sensors, computers and software to measure and/or control a particular variable [1, 12, 13, 14, 15, 16, 17, 18, 8, 19].

For small aircraft systems, as considered in this paper, multiple hardware redundancy is harder to achieve due to lack of operating space. Such schemes would also be costly and very complex to engineer and maintain.

Analytical redundancy makes use of a mathematical model of the monitored process and is therefore often referred to as the *model–based* approach to Fault Detection and Isolation (FDI). The model–based FDI is normally implemented in software form as a computer algorithm.

The fault diagnosis of aircraft or aerospace systems has become a very active research topic for theoretical and practical reasons. As an example, special sessions on fault diagnosis in aircraft systems in the recent *IFAC Symposium ACA 2004* [20] has covered most international research activities on this topic. A number of investigators have studied the use of analytical redundancy methods for FDI in aircraft and aerospace systems and several papers cover most of the previous and current research programs.

It is worth noting how all model–based methods use a model of the monitored system to produce residuals for fault detection and isolation. If the system is described accurately by the mathematical model, FDI is very straightforward. In real complex systems, however, modelling uncertainty arises inevitably for example process noise, turbulence, parameter variations and modelling errors. The detection of incipient faults presents a challenge to model–based FDI techniques due to unseparatable mixture between fault effects and modelling uncertainty [21, 22, 12, 15, 16, 17, 23, 18].

An important approach to achieve robustness in dynamic process FDI is the use of optimisation to minimise the effect of modelling uncertainty, whilst

maximising some fault effects.

In order to achieve robust FDI solutions, intelligent techniques [24, 25, 26] or adaptive methods [27, 3, 28, 29] can also be exploited.

Although many approaches have been developed, robust FDI for the case of aircraft systems and aerospace applications is still an open problem for further research.

This work deals with the residual generator design for the FDI of on–board sensors of a general aviation aircraft subject to disturbance signals (wind gusts) and measurement noise processes.

The system under diagnosis is modelled in terms of input–output polynomial description, so that the design of disturbance de–coupled residual generators can be reduced to the determination of the null–space of a specific polynomial matrix associated to the process model. In particular, the use of input–output forms allows to design in a straightforward fashion the analytical description for the disturbance de–coupled residual generators.

These dynamic fault detection filters, organised into bank structures, are able to achieve fault isolation properties. An appropriate choice of their parameters allows to maximise robustness with respect to both measurement noise and modelling errors, while optimising fault sensitivity characteristics.

The proposed FDI approach has been applied to a non–linear model of a PIPER PA30 aircraft. The residual generators have been designed on the basis of linearised models in different flight conditions and experimented with the data from non–linear flight simulator, implemented in Matlab/Simulink® environment. With respect to the previous work [30] by the same authors, the flight simulator has been improved in order to take into account the model of the measurement sensors and a Dryden turbulence description.

An important aspect of the approach to FDI suggested in this paper is the simplicity of structure of the technique used to generate the residual functions for detection and isolation, when compared with traditional schemes *e.g.* based on banks of unknown input observers (UIO) and Kalman filters [31, 32, 33].

The paper is organised as follows. The mathematical description of the monitored aircraft with the models of the input and output aircraft sensors are outlined in Section 2. Section 3 presents the approach exploited for the design of residual generators. Structural characteristics of such filters are also investigated in order to achieve disturbance de–coupling, sensitivity optimisation of the residual functions and robustness with respect to measurement

noise and modelling errors. Section 4 addresses the problem of the design of a bank of residual generators for the isolation of faults affecting the input and the output sensors. In order to show the effectiveness of the proposed filter design, the developed FDI scheme is applied to a model of a PIPER PA30 and some numerical results are reported in Section 5. Concluding remarks are finally summarised in Section 6.

2 Aircraft and Sensor Mathematical Description

V	True Air Speed (TAS)	δ_e	elevator deflection angle
α	angle of attack	δ_a	aileron deflection angle
β	angle of sideslip	δ_r	rudder deflection angle
P	roll rate	δ_{th}	throttle aperture percentage
Q	pitch rate	X,Y	horizontal coordinates
R	yaw rate		(inertial reference system)
ϕ	bank angle	H	altitude
θ	elevation angle		(inertial reference system)
ψ	heading angle	γ	flight path angle
n	engine shaft angular rate	m	airplane mass
$\begin{bmatrix} I_x & 0 & -I_{xz} \\ 0 & I_y & 0 \\ -I_{xz} & 0 & I_z \end{bmatrix}$		airplane inertia moments matrix	
F_x, F_y, F_z		total force components along body axes	
M_x, M_y, M_z		total moment components along body axes	
V_{Ax}, V_{Ay}, V_{Az}		inertial velocity components of the atmosphere	

Table 1: Nomenclature

The mathematical synthesis model of the PIPER PA30 is a classical non–linear six degrees of freedom aircraft model (rigid body), whose motion occurs as a consequence of applied forces and moments (aerodynamic, thrust and gravitational). A set of local approximations for this forces has been computed and scheduled depending on the values assumed by True Air Speed (TAS), flap, altitude, curve radius and flight path angle. In this way, it

is possible to obtain a mathematical model for each flight condition. This model is suitable for a state–space representation, as it can be made explicit.

The parameters in the analytic representation of the aerodynamic actions have been obtained from wind tunnel experimental data, as reported in [34, 35], and the aerodynamic actions are expressed along the axes of the wind reference system.

The non–linear model is given by following relations (using nomenclature of Table 1):

$$
\begin{aligned}
\dot{V} &= F_x \frac{\cos\alpha\cos\beta}{m} + F_y \frac{\sin\beta}{m} + F_z \frac{\sin\alpha\cos\beta}{m} \\
\dot{\alpha} &= \frac{-F_x \sin\alpha + F_z \cos\alpha}{mV\cos\beta} + Q - (P\cos\alpha + R\sin\alpha)\tan\beta \\
\dot{\beta} &= \frac{-F_x \cos\alpha\sin\beta + F_y \cos\beta - F_z \sin\alpha\sin\beta}{mV} + P\sin\alpha + \\
&\quad -R\cos\alpha \\
\dot{P} &= \frac{M_x I_z + M_z I_{xz} + PQ\, I_{xz}\,(I_x - I_y + I_z)}{I_x I_z - I_{xz}^2} + \\
&\quad + \frac{QR\,(I_y I_z - I_{xz}^2 - I_z^2)}{I_x I_z - I_{xz}^2} \\
\dot{Q} &= \frac{M_y + PR\,(I_z - I_x) - P^2 I_{xz} + R^2 I_{xz}}{I_y} \\
\dot{R} &= \frac{M_x I_{xz} + M_z I_x + PQ\,(I_x^2 - I_x I_y + I_{xz}^2)}{I_x I_z - I_{xz}^2} + \\
&\quad + \frac{QR\, I_{xz}\,(-I_x + I_y - I_z)}{I_x I_z - I_{xz}^2} \\
\dot{\phi} &= P + Q\sin\phi\tan\theta + R\cos\phi\tan\theta \\
\dot{\theta} &= Q\cos\phi - R\sin\phi \\
\dot{\psi} &= \frac{Q\,\sin\phi + R\cos\phi}{\cos\theta} \\
\dot{H} &= V\cos\alpha\cos\beta\sin\theta - V\cos\theta(\,\sin\beta\sin\phi + \sin\alpha\cos\beta\cos\phi) - V_{Az}
\end{aligned}
$$

This synthesis model has been completed by means of a first order dynamic model of a 4–pistons aspirated engine with the throttle aperture as input and the thrust intensity as output. A mathematical description of gusts as air velocity components, w_u, w_v and w_w, along body axes has been also considered.

The linearised model used for FDI purposes embeds the linearisation of the synthesis model, of the engine, of the wind actions and of the guidance

variables H and ψ. Hence, it can be written as follows:

$$\dot{x}(t) = \mathrm{A}x(t) + \mathrm{B}c(t) + \mathrm{E}d(t) \tag{1}$$

with

$$\begin{array}{l} x(t) = \left[\begin{array}{cccccccccccc} \Delta V(t) & \Delta\alpha(t) & \Delta\beta(t) & \Delta P(t) & \Delta Q(t) & \Delta R(t) & \Delta\phi(t) & \Delta\theta(t) & \Delta\psi(t) & \Delta H(t) & \Delta n(t) \end{array} \right]^{\mathrm{T}} \\ c(t) = \left[\begin{array}{cccc} \Delta\delta_e(t) & \Delta\delta_a(t) & \Delta\delta_r(t) & \Delta\delta_{th}(t) \end{array} \right]^{\mathrm{T}} \\ d(t) = \left[\begin{array}{ccc} w_u(t) & w_v(t) & w_w(t) \end{array} \right]^{\mathrm{T}} \end{array} \tag{2}$$

where Δ denotes the variations of the considered variables and $c(t)$ and $d(t)$ are the control inputs and the disturbances, respectively. The output equation associated to the model of Eq. (1) is of the type $y(t) = C\,x(t)$ where the rows of C correspond to rows of the identity matrix, depending on the measured variables.

In the following, the mathematical description of the subsystems used by the simulator model are given.

Command Surfaces Deflection Measurements
It is assumed that the deflection angles δ_e, δ_a, δ_r and δ_{th} are acquired with a sample rate of 100Hz by means of potentiometers. These sensors are affected by errors modelled by two additive components: bias and white noise. The bias values and the variance of the noises are given in Table (2).

Table 2: Input sensor errors parameters.

Input sensor	**Bias**	**White Noise Std**
Elevator deflection angle	0.0052 rad	0.0053 rad
Aileron deflection angle	0.0052 rad	0.0053 rad
Rudder deflection angle	0.0052 rad	0.0053 rad
Throttle aperture	1%	1%

Angular Rate Measurement
It is assumed that the angular rate measures are given by a set of three gyroscopes of an Inertial Measurement Unit (IMU) with a sample rate of 100Hz.

The errors affecting this measurement unit can be classified as follows [36]:

- Errors due to non unitary scale factor, modelled by a multiplicative factor belonging to the range $[0.99, 1.01]$.
- Alignment error of spin axes with respect to body (reference) axes. These errors can be modelled by considering each spin axis oriented in a 3D space by means of an azimuth and elevation angle with respect to its reference axis. It this way, the alignment errors can be described by six error angles up to 1 deg. It is worth observing that the errors previously considered are generated by means of uniform random variables updated every simulation.
- Limited bandwidth of the considered gyro (10 Hz).
- g–sensitivity ($72\ \frac{deg}{h\ g}$).
- Additive white noise (216 deg/h).
- Gyro drift, described by a coloured stochastic process characterised by a standard deviation of 1080 deg/h and a decay time of 20 min.

Attitude Angle Measurement
The angles are actually generated by a digital filtering system based on a DSP that processes both the angular rate and the accelerations provided by the IMU with a sample rate of 100Hz.

The angle generation system has been considered equivalent to a mechanical vertical gyro for aeronautical purposes (artificial horizon). As reported in Chapter 11 of [37], the measurement errors are due to the sum of two causes:

- A systematic error generated by the apparent vertical. This effect cannot be neglected because the fault diagnosis, as it will be shown in the following, has to be performed in coordinated turn flight condition.
- A white noise modelling the imperfection of both the system and the environment influences.

The behaviour of this angle measurement system is such that the previous two effects are correlated by a first order filter system with time constant equal to 60 sec [37]. Therefore, the resulting attitude angle measurements

are affected by an additive coloured noise characterised by a standard deviation of 1 deg.

Air Data System (ADS)
It is assumed that the ADS unit consists of an Air Data Computer (ADC) providing measures with a sample rate of 1 Hz. The errors affecting the TAS can be classified as follows:

- Calibration error affecting the differential pressure sensor. This error leads to a TAS computation systematic error, performed the ADC, fulfilling the ARINC (Aeronautical Radio Inc.) [38] accuracy requirements (2 m/sec) [37].
- Additive coloured noise due to wind gusts (std 1 and correlation time 2.3 sec).
- Additive white noise (std 0.5 m/sec) modelling the imperfection of the system and the environment influences.

With regards to the altitude, errors can be classified as:

- Calibration error affecting the static pressure sensor. This error leads to an altitude computation systematic error, performed the ADC, fulfilling the ARINC accuracy requirements (5 m) [38];
- Additive White noise (std 1 m) modelling the imperfection of the system and the environment influences.

Heading Reference System (HRS)
This unit is assumed to consist of a magnetic compass coupled to a directional gyro. As reported in [37] the measurement errors are due to the sum of two causes:

- a systematic error generated by a bias of the magnetic compass (1 deg),
- a white noise modelling the imperfection of the system and the environment influences.

The behaviour of the HRS system is such that the two previous effects are correlated by a first order filter with time constant equal to 60 sec [37]. Hence, the resulting heading measurement is affected by an additive coloured noise characterised by a std 1 deg.

Engine Shaft Rate Measurement
The engine shaft rate is measured by mean of an incremental encoder whose errors are modelled as a white noise. The quantisation error of the encoder is determined by a resolution of 10000 pulse/rev.

Servo Actuator Models
The servo–actuator description of elevator, aileron, rudder and throttle consist of second order linear models with saturations.

Dryden Atmosphere Model
The Dryden Turbulence Model block of the Aerospace Blockset of Matlab® 6.5 has been used. The Dryden spectral representation adds turbulence obtained by an appropriate forming filter excited by a band–limited white noise. This block implements the mathematical representation in the U.S. Military Specification MIL–F–8785C.

3 Residual Generator Design

Let us consider a linear, time–invariant, continuous–time system described by the following input–output equation in the form:

$$P(s)\, y(t) = Q(s)\, u(t), \tag{3}$$

where s is the derivative operator and $P(s)$ and $Q(s)$ are polynomial matrices with dimensions $(m \times m)$ and $(m \times \ell)$ respectively, with $P(s)$ nonsingular. The terms $u(t)$ and $y(t)$ are the ℓ–dimensional and m–dimensional input and output vectors of the considered multivariable system.

Models of type (3) can be frequently found in practice by applying well–known physical laws to describe the input–output dynamical links of various systems and are a powerful tool in all fields where the knowledge of the system state does not play a direct role, such as residual generator design, identification, de–coupling, output controllability, etc. Algorithms to transform

state–space models to equivalent input–output polynomial representations and vice versa are available [39].

In order to design the residual generators, $Q(s)$ can be decomposed according to the following structure:

$$P(s)\,y(t) = \left[\begin{array}{ccc} Q_c(s) & Q_d(s) & Q_f(s) \end{array}\right] \left[\begin{array}{c} c(t) \\ d(t) \\ f(t) \end{array}\right] \tag{4}$$

where $c(t)$ is the ℓ_c–dimensional known–input vector, $d(t)$ is the ℓ_d–dimensional disturbance vector, $f(t)$ is the ℓ_f–dimensional monitored fault vector and $\ell_c + \ell_d + \ell_f = \ell$.

A general linear residual generator for the fault detection process of system (4) is a filter of type:

$$R(s)\,r(t) = S_y(s)\,y(t) + S_c(s)\,c(t) \tag{5}$$

that processes the known input–output data and generates the residual $r(t)$, *i.e.* a signal which is "small" (ideally zero) in the fault–free case and is "large" when a fault is acting on the system.

Without loss of generality, $r(t)$ can be assumed to be a scalar signal. In such condition $R(s)$ is a polynomial with degree greater than or equal to the row–degree of $S_c(s)$ and $S_y(s)$, in order to guarantee the physical realisability of the filter.

An important aspect of the design concerns the de–coupling of the disturbance $d(t)$ to produce a correct diagnosis in all operating conditions.

Equation (4) can be rewritten in the form:

$$P(s)\,y(t) - Q_c(s)\,c(t) - Q_f(s)\,f(t) = Q_d(s)\,d(t)\,. \tag{6}$$

Premultiplying all the terms in (6) by a row polynomial vector $L(s) \in \mathcal{N}_\ell(Q_d(s))$, that is to the left null–space of $Q_d(s)$, we obtain:

$$L(s)\,P(s)\,y(t) - L(s)\,Q_c(s)\,c(t) - L(s)Q_f(s)\,f(t) = 0\ . \tag{7}$$

Starting from Eq. (7) with $f(t) = 0$, it is possible to obtain a residual generator of type (5) by setting:

$$\begin{array}{rcl} S_y(s) & = & L(s)\,P(s) \\ S_c(s) & = & -L(s)\,Q_c(s) \\ R(s) & = & (1+\tau_1 s)(1+\tau_2 s)..(1+\tau_{n_f} s) = \\ & = & a_1 s^{n_f} + a_2 s^{n_f-1} + .. + 1\ , \end{array} \tag{8}$$

where n_f is the maximal row–degree of the pair $\{L(s)\,P(s),\ L(s)\,Q_c(s)\}$. The polynomial $R(s)$ can be arbitrarily selected. The choice $R(s) = (1+\tau_1 s)(1+\tau_2 s)\ldots(1+\tau_{n_f} s)$ leads to an asymptotically stable filter when the real parts of the n_f roots $1/\tau_i (i = 1, 2, \ldots, n_f)$ are negative. In this way, in absence of fault, equation (7) can be rewritten also in the form:

$$R(s)\,r(t) = L(s)\,P(s)\,y(t) - L(s)\,Q_c(s)\,c(t) = 0\,. \tag{9}$$

When a fault is acting on the system the residual generator is governed by the relation:

$$R(s)\,r(t) = L(s)\,Q_f(s)\,f(t) \tag{10}$$

and $r(t)$ assumes values that are different from zero if $L(s)$ does not belong to the $\mathcal{N}_\ell(Q_f(s))$.

In order to determine all possible residual generators of minimal order it is necessary to transform Eq. (3) into a minimal input-output polynomial representation, that is an equivalent representation with the polynomial matrix $P(s)$ row reduced [40]:

$$P(s) = D(s)\,N + E(s), \tag{11}$$

where $D(s) = \mathrm{diag}\,[s^{\nu_1}, s^{\nu_2}, \ldots, s^{\nu_m}]$ and the highest–row–degree coefficient matrix N is non singular.

In this condition the integers ν_i represent the set of the Kronecker output invariants associated to the pair $\{A,\, C\}$ of every observable realization of $\{P(s),\, Q(s)\}$ in the state-space. This step can be omitted if the designer is not interested in using minimal order residual generators.

Moreover, it is necessary to compute a minimal basis of $\mathcal{N}_\ell(Q_d(s))$. Under the assumption that matrix $Q_d(s)$ is of full normal rank, *i.e.* $\mathrm{rank}\,Q_d(s) = \ell_d$, $\mathcal{N}_\ell(Q_d(s))$ has dimension $m - \ell_d$ and a minimal basis of such subspace can be computed as suggested in [40].

It can be noted that in absence of disturbances $\ell_d = 0$, so that $\mathcal{N}_\ell(Q_d(s))$ coincides with the whole vector space. Consequently, a set of residual generators for system (4) with $f(t) = 0$ can be expressed as

$$\begin{array}{rcc} R_{ri}(s)\,r_i(t) & = & P_{ri}(s)\,y(t) - Q_{c_{ri}}(s)\,c(t) \\ & & (i = 1, 2, \ldots, m), \end{array} \tag{12}$$

where $P_{ri}(s)$ and $Q_{c_{ri}}(s)$ are the i–th rows of matrices $P(s)$ and $Q_c(s)$, respectively, ν_i is the degree of $P_{ri}(s)$ and $R_{ri}(s)$ is an arbitrary polynomial

with degree equal to ν_i and with all the roots with negative real part. Since $Q_{c_{ri}}(s)$ cannot show a degree greater than ν_i, the physical realisability of the residual generator is guaranteed.

In general, for $0 < \ell_d < m$ matrix $Q_d(s)$ can be partitioned in the following way:

$$Q_d(s) = \left[\begin{array}{c} Q_{d_1}(s) \\ Q_{d_2}(s) \end{array} \right] , \tag{13}$$

where matrices $Q_{d_1}(s)$ and $Q_{d_2}(s)$ have dimension $\ell_d \times \ell_d$ and $(m - \ell_d) \times \ell_d$ respectively.

It can be assumed, without loss of generality, that matrix $Q_{d_1}(s)$ is non singular. In this case it can be easily verified that a basis of $\mathcal{N}_\ell(Q_d(s))$ is given by the polynomial matrix:

$$\begin{array}{rl} B(s) = & [Q_{d_2}(s) \operatorname{adj} Q_{d_1}(s) \dots \\ & -\det Q_{d_1}(s)\, I_{m-\ell_d}], \end{array} \tag{14}$$

by assuming $\operatorname{adj} Q_{d_1}(s) = 1$ for $\ell_d = 1$.

By partitioning $P(s)$ and $Q_c(s)$ as $Q_d(s)$ in (13):

$$P(s) = \left[\begin{array}{c} P_1(s) \\ P_2(z) \end{array} \right] \qquad Q_c(s) = \left[\begin{array}{c} Q_{c_1}(s) \\ Q_{c_2}(s) \end{array} \right], \tag{15}$$

a basis (not necessarily of minimal order) of the residual generators (5) for the system (4) with $f(t) = 0$ is obtained by replacing in relation (8) the row polynomial vector $L(s)$ with the polynomial matrix $B(s)$, *i.e.*:

$$\begin{array}{rcl} S_y(s) & = & Q_{d_2}(s) \operatorname{adj} Q_{d_1}(s)\, P_1(s) + \\ & & -\det Q_{d_1}(s)\, P_2(s) \\ S_c(s) & = & -Q_{d_2}(s) \operatorname{adj} Q_{d_1}(s)\, Q_{c_1}(s) + \\ & & +\det Q_{d_1}(s)\, Q_{c_2}(s) \\ R(s) & = & \operatorname{diag}\left[R_1(s) R_2(s) \dots R_{m-\ell_d}(s)\right] , \end{array} \tag{16}$$

where the degree of the polynomial $R_i(s)$ is n_{f_i} $(i = 1, \dots, m - \ell_d)$, that is the degree of the $i - th$ row of the matrix $S_y(s)$.

Remark 1 *By denoting with n_f^* the minimal value of the integers n_{f_i} $(i = 1, \dots, m-\ell_d)$ it is easy to prove that the order n_f^* of a minimal order residual generator for the system (4) is constrained in the following range:*

$$\nu_{\min} \;\leq\; n_f^* \;\leq\; (\ell_d + 1)\, \nu_{\max} \tag{17}$$

where $\nu_{\min}$ and $\nu_{\max}$ are the least and the greatest Kronecker invariant respectively.
The lower bound can be obtained in the no–disturbance case ($\ell_d = 0$) from relation (12) by selecting the row of $P(s)$ associated to the least Kronecker invariant. The upper bound can be obtained by taking into account the maximal degree of the polynomials of the matrices. A similar result, obtained with a different approach can be found in [41, 42].

The diagnostic capabilities of a residual generator of the type of Eqs. (9) and (10) strongly depend on an accurate choice of the terms $L(s)$ and $R(s)$. The design freedom in the selection of the matrix $L(s)$, when $m - \ell_d > 1$, can be used to optimise the sensitivity properties of $r(t)$ to the fault $f(t)$, for example by maximising the steady–state gain of the transfer function $L(s)\,Q_f(s)/R(s)$ given in Eq. (10). By denoting with $b_i(s)(i = 1, 2, \ldots, m - \ell_d)$ the row vectors of the basis $B(s)$ of the $\mathcal{N}_\ell(Q_d(s))$, $L(s)$ can be chosen as a linear combination of these vectors:

$$L(s) = \sum_{i=1}^{m-\ell_d} k_i b_i(s), \tag{18}$$

with the real constants k_i which maximise:

$$\lim_{s\to 0} \frac{1}{R(s)} [\sum_{i=1}^{m-\ell_d} k_i b_i(s)]\, Q_f(s) = [\sum_{i=1}^{m-\ell_d} k_i b_i(0)]\, Q_f(0) \tag{19}$$

under the constraint

$$\sum_{i=1}^{m-\ell_d} k_i^2 = 1. \tag{20}$$

In this way, when the fault $f(t)$ is a step–function of magnitude F, it results:

$$\lim_{t\to\infty} r(t) = \lim_{s\to 0} s \frac{L(s)Q_f(s)}{R(s)} \frac{F}{s} = [\sum_{i=1}^{m-\ell_d} k_i b_i(0)]\, Q_f(0)\, F. \tag{21}$$

Another design choice regards the location of the roots of the polynomial $R(s)$ in the left–half s–plane, which influences the transient characteristics (maximum overshoot, delay time, rise time, settling time, etc.) of the filter of Eq. (10) with respect to unit–step response. In many applications these characteristics must be kept within tolerable or prescribed limits in order to

guarantee good performance of the filter in terms of fault detection times and false alarm identification. This leads to define a reference transfer function $G_r(s)$ and an approximation criterion in order to obtain, with an appropriate choice of $R(s)$, a satisfactory similarity between the frequency responses of the two filters $G_r(s)$ and $G_f(s) = L(s)Q_f(s)/R(s)$, that is

$$\frac{|G_f(j\omega)|^2}{|G_r(j\omega)|^2} = 1, \tag{22}$$

for every ω belongs to a given frequency range.

Moreover, it is important to note that, in general, the requirement of fast transient responses for disturbance de–coupling residual generators can lead to large bandwidths. As a consequence, residual generator robustness with respect to both input–output measurement noises and modelling errors might deteriorate.

On the other hand, the design of the fault detection and isolation scheme must take into account the knowledge of the frequency spectra of such signals, by achieving, if necessary a good compromise solution among the different specifications that have to be satisfied.

Remark 2 *Finally, it must be noted that Eq. (4) considers also the cases of additive faults on the input and output sensors, $f_c(t)$ and $f_o(t)$ respectively. In this situations only the measurements:*

$$c^*(t) = c(t) + f_c(t)\,, \tag{23}$$

$$y^*(t) = y(t) + f_o(t)\,, \tag{24}$$

are available for the residual generators so that Eq. (9) becomes:

$$R(s)\,r(t) = L(s)\,P(s)\,y^*(t) - L(s)\,Q_c(s)\,c^*(t) = 0 \tag{25}$$

in absence of faults and

$$R(s)\,r(t) = L(s)\,Q_c(s)\,f_c(t) - L(s)\,P(s)\,f_o(t) \tag{26}$$

when faults on input-output sensors are considered.

4 Residual Generation for Fault Isolation

This section addresses the problem of the design of a bank of residual generators for the isolation of faults affecting the input and output sensors. The design is performed by using the disturbance de–coupling method suggested in the previous section. It is assumed in the following that $m > \ell_d + 1$.

To univocally isolate a fault concerning one of the *input sensors*, under the hypotheses that the remaining input sensors and all output sensors are fault–free, a bank of residual generator filters is used, according to Figure (1).

The number of these generators is equal to the number ℓ_c of system control inputs, and the i–th device ($i = 1, \ldots, \ell_c$) is driven by all but the i–th input and all the outputs of the system.

In this case, a fault on the i–th input sensor affects all but the i–th residual generator.

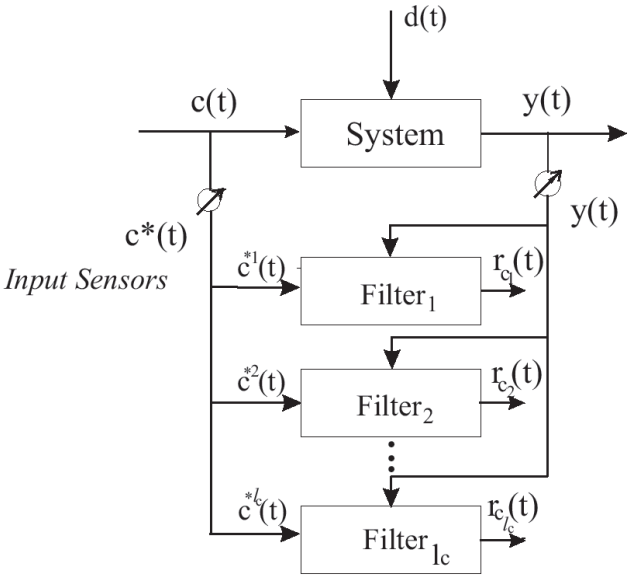

Figure 1: Scheme for input sensor fault isolation.

With reference to Figure (1), $c^{*i}(t)$ represents the $\ell_c - 1$ dimensional vector

obtained by deleting from $c^*(t)$ the i–th component, and

$$c^*(t) = c(t) + f_{c_i}(t)\,, \tag{27}$$

with

$$f_{c_i}(t) = \left[\begin{array}{ccccccc} 0 & \ldots & 0 & h_{c_i}(t) & 0 & \ldots & 0 \end{array}\right]^T . \tag{28}$$

Note that $c^{*i}(t) = c^i(t)$ when the fault on the i–th input sensor $h_{c_i}(t)$ is considered.

In these conditions, Eq. (6) of the system becomes:

$$P(s)\,y(t) \;= Q_c(s)\,c(t) \;+\; Q_d(s)\,d(t) + q_{c_i}(s)\,h_{c_i}(t)\,, \tag{29}$$

where $q_{c_i}(s)$ represents the i–th column of the matrix $Q_c(s)$.

Hence, by multiplying Eq. (29) by the matrix $L_{c_i}(s)$, where $L_{c_i}(s)$ is a row vector belonging to the basis for the left null space of the matrix $[Q_d(s)\,|\,q_{c_i}(s)]$, and $Q_c^i(s)$ is the matrix obtained by deleting from $Q_c(s)$ the i–th column, the equation of the i–th filter becomes:

$$R_{c_i}(s)\,r_{c_i}(t) = L_{c_i}(s)\,P(s)\,y(t) - L_{c_i}(s)\,Q_c^i(s)\,c^{*i}(t) \;=\; 0, \tag{30}$$

while, for the j–th filter, with $j \neq i$, it results:

$$\begin{array}{l} R_{c_j}(s)\,r_{c_j}(t) = L_{c_j}(s)\,P(s)\,y(t) - L_{c_j}(s)\,Q_c^j(s)\,c^{*j}(t) = \\ = L_{c_j}(s)\,q_{c_i}(s)\,h_{c_i}(t). \end{array} \tag{31}$$

$R_{c_i}(s)$ and $R_{c_j}(s)$ are arbitrary polynomials with all the roots with negative real part.

In a similar way, in order to univocally isolate a fault concerning one of the *output sensors*, under the hypotheses that all the input sensors and the remaining output sensors are fault–free, a bank of residual generator filters is used, according to Figure (2).

The number of these generators is equal to the number m of system outputs, and the i–th device ($i = 1, \ldots, m$) is driven by all but the i–th output and all the inputs of the system. In this case, a fault on the i–th output sensor affects all but the i–th residual generator.
With reference to Figure (2), $y^{*i}(t)$ represents the $m-1$ dimensional vector obtained by deleting from $y^*(t)$ the i–th component, where

$$y^*(t) = y(t) + f_{o_i}(t) \tag{32}$$

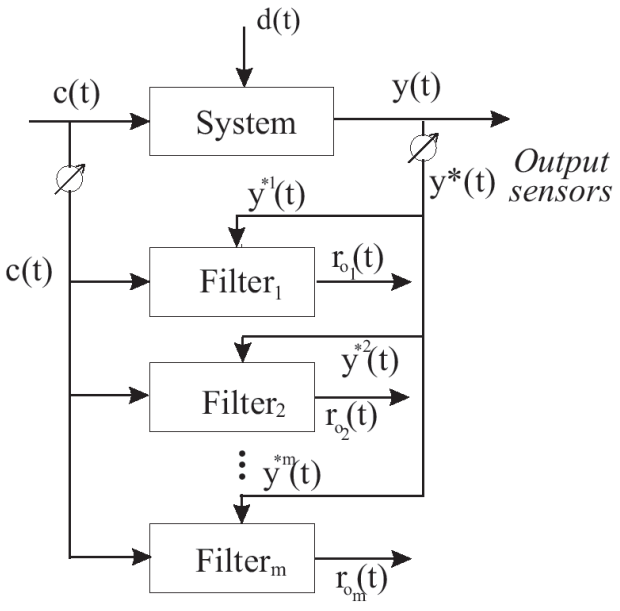

Figure 2: Bank of residual generators for output sensor fault isolation.

and with

$$f_{o_i}(t) = \left[\begin{array}{ccccccc} 0 & \dots & 0 & h_{o_i}(t) & 0 & \dots & 0 \end{array} \right]^T . \tag{33}$$

In these conditions, Eq. (6) of the system becomes:

$$P(s)\, y(t) \; = Q_c(s)\, c(t) \; + \; Q_d(s)\, d(t) - p_i(s)\, h_{o_i}(t)\,, \tag{34}$$

where $p_i(s)$ represents the i–th column of the matrix $P(s)$.

Note that $y^{*i}(t) = y^i(t)$ when a fault on the i–th output sensor $h_{o_i}(t)$ is considered.

Hence, by multiplying Eq. (34) by the matrix $L_{o_i}(s)$, where $L_{o_i}(s)$ is a row vector belonging to the basis for the left null space of the matrix $[Q_d(s) \,|\, p_i(s)]$, and denoting $P^i(s)$ the matrix obtained by deleting from $P(s)$ the i–th column, the equation of the i–th filter becomes:

$$R_{o_i}(s)\, r_{o_i}(t) = L_{o_i}(s)\, P^i(s)\, y^{*i}(t) - L_{o_i}(s)\, Q_c(s)\, c(t) \; = \; 0, \tag{35}$$

while, for the j–th filter, with $j \neq i$, it results:

$$R_{o_j}(s)\, r_{o_j}(t) = L_{o_j}(s)\, P^j(s)\, y^{*j}(t) - L_{o_j}(s)\, Q_c(s)\, c(t) = \tag{36}$$

$$= -L_{o_j}(s)\, p_i(s)\, h_{o_i}(t). \tag{37}$$

$R_{o_i}(s)$ and $R_{o_j}(s)$ are arbitrary polynomials whose roots have negative real part.

In order to summarise the FDI capabilities of the presented schemes, Table (3) shows the "fault signatures" in case of a single fault in each input and output sensor.

The residuals which are affected by input and output faults are marked with the presence of '1' in the correspondent table entry, while an entry '0' means that the input or output fault does not affect the correspondent residual.

Table 3: Fault signatures.

Residual / Fault	f_{c_1}	f_{c_2}	$\dots$	$f_{c_{\ell_c}}$	f_{o_1}	f_{o_2}	$\dots$	f_{o_m}
r_{c_1}	0	1	$\dots$	1	1	1	$\dots$	1
r_{c_2}	1	0	$\dots$	1	1	1	$\dots$	1
$\vdots$	$\vdots$	$\vdots$	$\vdots$	$\vdots$	$\vdots$	$\vdots$	$\vdots$	$\vdots$
$r_{c_{\ell_c}}$	1	1	$\dots$	0	1	1	$\dots$	1
r_{o_1}	1	1	$\dots$	1	0	1	$\dots$	1
r_{o_2}	1	1	$\dots$	1	1	0	$\dots$	1
$\vdots$	$\vdots$	$\vdots$	$\vdots$	$\vdots$	$\vdots$	$\vdots$	$\vdots$	$\vdots$
r_{o_m}	1	1	$\dots$	1	1	1	$\dots$	0

All the elements out of the main diagonal on Table (3) are '1's when both the following conditions hold:

- For $i = 1, \dots, \ell_c$, the column vectors of the matrix $Q_c^i(s)$ and the column vectors of the matrix $P(s)$ are not orthogonal with the row vector $L_{c_i}(s)$.
- For $j = 1, \dots, m$, the column vectors of the matrix $P^j(s)$ and the column vectors of the matrix $Q_c(s)$ are not orthogonal with the row vector $L_{o_j}(s)$.

It is important to note that when not all the elements out of the main diagonal of the Table (3) are '1's, the fault isolation is still feasible if the columns of the fault signature table are all different from each other.

Moreover, it is worth noting that when $m - (\ell_d + 1) > 1$, all the bases of the left null space of the matrices $[Q_d(s) \,|\, q_{c_i}(s)]$ and $[Q_d(s) \,|\, p_i(s)]$ have

dimension bigger than 1. In these conditions, the degrees of freedom in the choice of the vectors $L_{c_i}(s)$ and $L_{o_i}(s)$ belonging to the left null space can be used as described in Section (3).

5 Experimental Results

To show the diagnostic characteristics brought by the application of the proposed fault detection and isolation scheme to the the general aviation PIPER PA–30 aircraft model addressed in Section 2, some numerical results obtained in the Matlab/Simulink® environment are reported here.

The design of the disturbance de–coupling residual generators described in Section 3 and 4 for input and output sensor FDI has been performed by considering the linearised model for the aircraft presented at the end of Section 2. Such linearised model of the aircraft corresponds to a flight condition, that can be a branch of a more complex trajectory, described by:

- radius of curvature: 1000 m
- speed: $V = 50\ \frac{m}{sec}$
- altitude: $H = 330$ m
- flap: $= 0^o$.

The residual generator filters are therefore fed by the 4 component input vector $c(t)$ and the 9 component output vector $y(t)$ acquired from the non–linear dynamic aircraft model described in Section 2 and simulated in the Matlab/Simulink® environment. Moreover, the input and output sequences are affected by the measurement errors obtained from the aircraft instrument models presented in Section 2.

In particular, as presented in Section 3, a bank of 4 residual generator filters has been used to detect input sensor faults regarding the 4 input control variables $c(t) = [\Delta\delta_e(t), \Delta\delta_a(t), \Delta\delta_r(t), \Delta\delta_{th}(t)]^T$.

Moreover, in order to obtain the fault *isolation* properties recalled in Section 4, each residual generator function of the considered bank is fed by all but one the 4 control input signals and by the 9 output variables $y(t) = [\Delta V(t), \Delta P(t), \Delta Q(t), \Delta R(t), \Delta\phi(t), \Delta\theta(t), \Delta\psi(t), \Delta H(t), \Delta n(t)]^T$. The output variables $\Delta\alpha(t)$ and $\Delta\beta(t)$ were not considered as their measurements are critical to obtain.

Hence, each filter of the bank is independent of one of the 4 input signals and then is also insensitive to the corresponding fault signals. Obviously, as presented in Section 3, the residual generator bank has been designed to be de–coupled from 3 wind gust signals $d(t) = [w_u(t), w_v(t), w_w(t)]^T$, that represent disturbance terms acting on the aircraft system. On the other hand, the capabilities of the FDI system are hence related to the properties of the residual generator functions in the presence of measurement errors, modelling approximations and disturbance signals that cannot be completely de–coupled.

However, the robustness properties of the filters in terms of fault sensitivity and disturbance insensitivity can be achieved according to Section 3. The synthesis of the dynamic filters for FDI has been performed by choosing a suitable linear combination of residual generator functions that maximise the steady–state gain of the transfer functions of Eqs. (31) between input sensor fault signals $f_{c_i}(t)$ and residual functions $r_{c_j}(t)$ $(i, j = 1, \ldots, 4,\ j \neq i)$. Moreover, for each residual generator, the roots of the polynomial $R_{c_j}(s)$ have been optimised numerically [43] in order to obtain suitable transient dynamics.

In order to assess the technique for diagnosing input and output sensor faults, aircraft operating conditions with different faults were simulated by using the non–linear dynamic model of the system. Faults in single input–output sensors have been generated by producing positive and negative variations in the input–output signals $c(t)$ and $y(t)$.

The residual signals indicate fault occurrence according to whether their values are lower or higher than the thresholds fixed in fault–free conditions. The threshold values depend on the residual error amount due to measurement errors, linearised model approximations and disturbance signals that are not completely de–coupled. A margin of 10% between the positive and negative thresholds and the maximum and minimum values of the fault–free residual signals were respectively imposed, as shown in Figure (3).

As an example, the 4 residual functions $r_{c_i}(t)$ generated by the filter bank for input sensor fault isolation, under both fault–free and faulty conditions are shown in Figure (3).

Continuous lines represent the fault–free residual functions, while the dotted lines depict the faulty residual signals. As depicted in Figure (3), the fault has been generated on the 1st input sensor of the considered aircraft, commencing at time $t = 150$s.

It is worth noting that the first residual function of Figure (3), for the

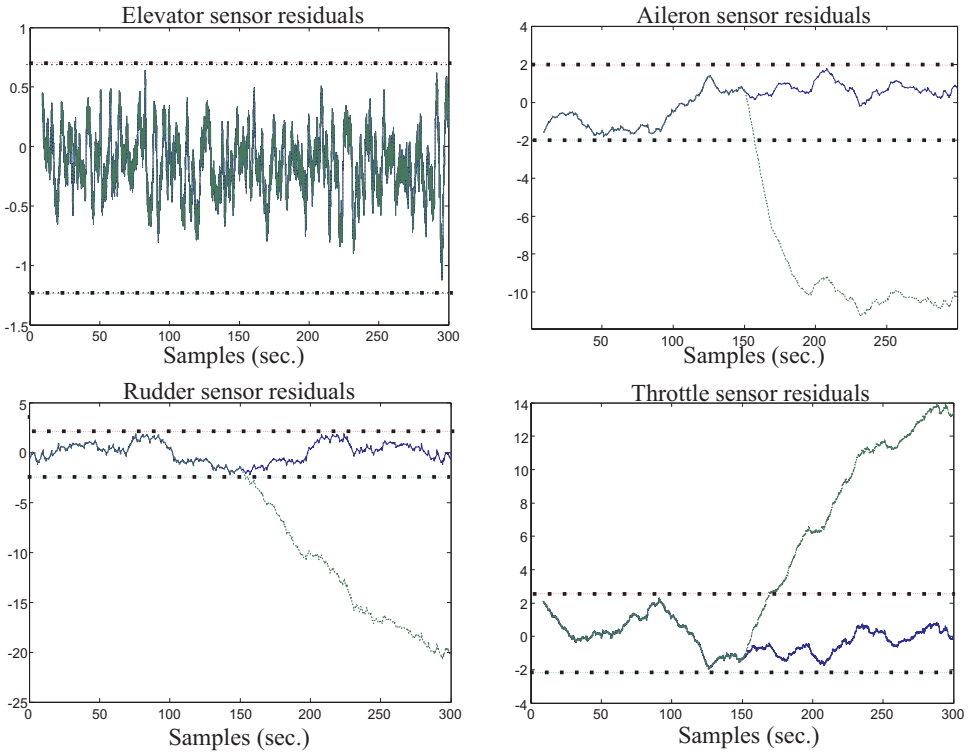

Figure 3: Bank residuals for the 1st input sensor fault $f_{c_1}(t)$ isolation.

isolation of a fault regarding the considered input sensor $f_{c_1}(t)$, does not depend on a fault affecting the input sensor itself, as the corresponding residual $r_{c_1}(t)$ filter has been designed to be sensitive to the input signal $c^{*1}(t)$.

The optimisation of the filter parameters, *i.e.* the values of the roots $-1/\tau_i (i = 1, 2, \ldots, n_f)$ and of real constants k_i, were obtained by means of the *Genetic Algorithm Optimisation Toolbox* (GAOT) [43] for Matlab®, as it seems to be able to manage the well–known local minima problems.

In particular, in this case, the roots of the $R_{c_i}(s)$ polynomial matrix have been optimised and placed in a range between -1 and -10^{-2} in order to maximise the fault detection promptness, as well as to minimise the occurrence of false alarms.

In the same way, the 9 residual functions $r_{o_j}(t)$ have been generated by the filter bank for the output sensor fault isolation and the results are shown in Figure (4).

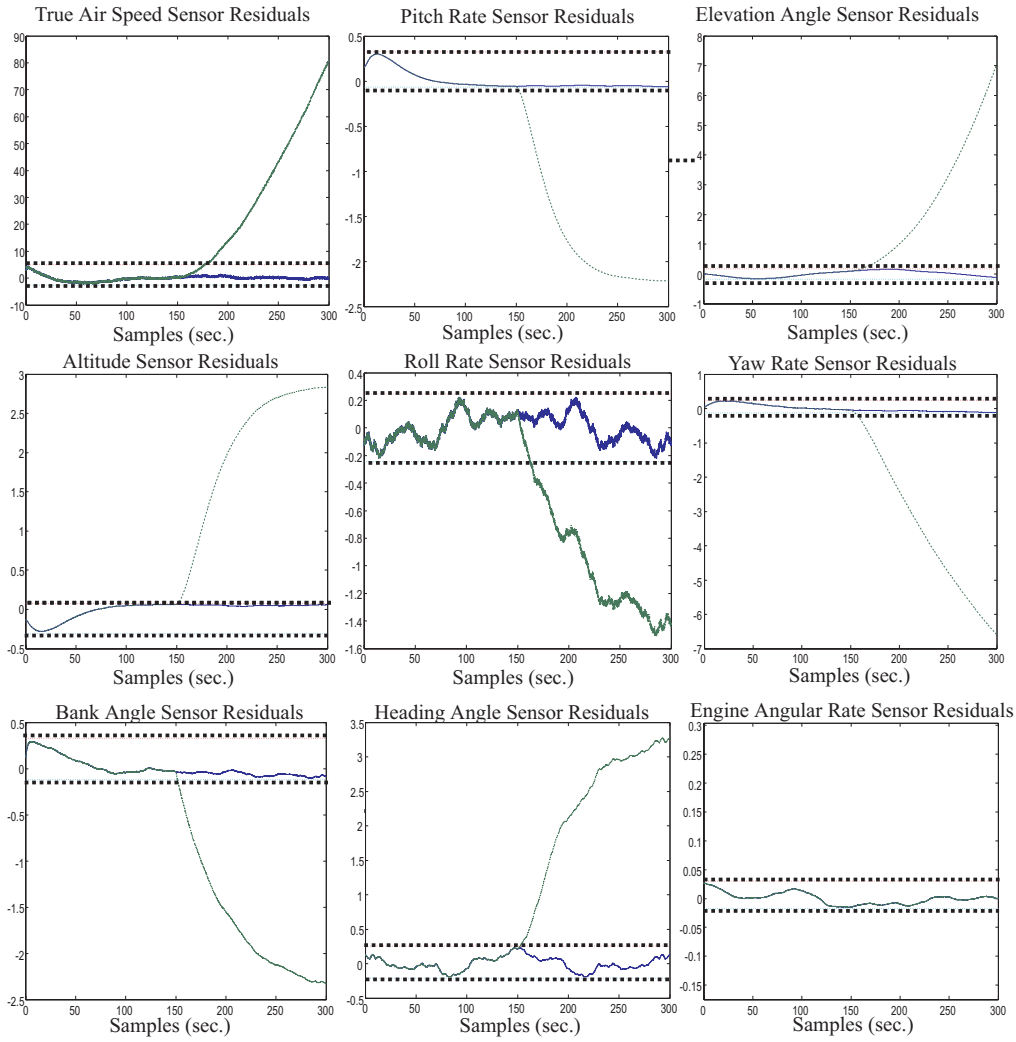

Figure 4: Residuals of the bank for the isolation of the 9^{th} output sensor fault $f_{o_9}(t)$.

In Figure (4) continuous lines represent the fault–free residual functions, while the dotted lines depict the faulty residual signals. As depicted in Figure (4), the fault has been generated on the 9^{st} output sensor of the considered aircraft, commencing at time $t = 150$s.

In order to determine the range out of which the input and output sensor faults are detectable, the maximum and minimum values assumed by the

$r_{c_i}(t)$ and $r_{o_j}(t)$ functions in fault–free conditions must be computed with an acceptable false–alarms rate.

To summarise the performance of the FDI technique, the minimal detectable step faults on the various sensors are collected in Tables (4) and (5).

In particular, Table (4) collects the minimal detectable *step* fault amplitudes simulated on the *input* sensors, when $r_{c_j}(t)$ is monitored in order to perform the isolation of the considered fault case $f_{c_i}(t)$ $(i, j = 1, \ldots, 4, i \neq j)$.

Table 4: Minimal detectable step input sensor faults.

Input Sensor Variable $c_i(t)$	**Fault Size**	**Detection Delay**
Elevator deflection angle	2^o	18 sec
Aileron deflection angle	3^o	6 sec
Rudder deflection angle	4^o	8 sec
Throttle aperture %	2%	15 sec

In the same way, Table (5) collects the minimal detectable *step* fault amplitudes on the *output* sensors, when $r_{o_j}(t)$ is monitored in order to perform the isolation of the considered output sensor fault case $f_{o_i}(t)$ $(i, j = 1, \ldots, 9, i \neq j)$.

Table 5: Minimal detectable step output sensor faults.

Output Sensor Variable $y_i(t)$	**Fault Size**	**Detection Delay**
True Air Speed	8 m/sec	27 sec
Pitch Rate	3 deg/sec	22 sec
Elevation Angle	5 deg	28 sec
Altitude	8 m	12 sec
Roll Rate	2 deg/sec	24 sec
Yaw Rate	3 deg/sec	29 sec
Bank Angle	5 deg	5 sec
Heading Angle	6 deg	25 sec
Engine Angular Rate	20 RPM	30 sec

The minimal detectable fault values in Tables (4) and (5) are expressed in the unit of measure of the sensor signals and are relative to the case in which

the occurrence of a fault must be detected and isolated as soon as possible.

The detection delay time, reported in Tables (4) and (5), is evaluated on the basis of the time taken by the slowest residual function to cross the settled threshold.

Finally, the performance of the residual generators seems to assess the diagnostic capabilities of the suggested technique, that has been tested also with different fault models (*e.g.* small and large bias with ramp transients [31] as well as intermittant faults). Moreover, the proposed strategy for the FDI on the input and output sensors appear to be promising for diagnostic application to general aviation aircrafts.

It is important to note that similar results could be obtained by means of equivalent dynamic observers, UIO or Kalman filters, even if the corresponding realisation could require a more complex design and an higher cost implementation.

6 Conclusion

The paper has provided interesting results in the detection and isolation of faults on the sensors of a non–linear aircraft system by using a model–based approach.

The example reported shows that different types of fault which have a barely detectable effect on anyone measurement, can be detected easily using a bank of residual generator in the form of dynamic filters.

An important aspect of the approach suggested in this paper to FDI is the simplicity of structure of the technique used to generate the residual functions for detection and isolation, when compared with traditional schemes *e.g.* based on banks of Unknown Input Observers (UIO) and Kalman filters. Although the method outlined focuses to some extent on input–output or state–space concepts, the actual algorithm for use in the real–time on–board application is based only on input–output processing of all measurable signals, *i.e.* all measurements as well as control signals.

The algorithmic simplicity is a very important aspect when considering the need for verification and validation of a demonstrable scheme for air–worthiness certification. The more complex the computations required to implement the scheme, the higher the cost and complexity in terms of certification. This aspect of the work together with the fact that the modelling uncertainty and the measurement noise have been very well tackled, serve to

highlight the potential of using such a method in real applications.

Further studies are being carried out to evaluate the effectiveness of the approach applied to real aircraft system data.

References

[1] R. Patton, "Fault detection and diagnosis in aerospace systems using analytical redundancy," in *IEE Computing & Control Engineering Journal*, vol. 2, pp. 127–136, 1990.

[2] R. J. Patton and J. Chen, "A review of parity space approaches to fault diagnosis for aerospace systems," *AIAA Journal of Guidance, Control & Dynamics*, vol. 17, no. 2, pp. 278–285, 1994.

[3] T. Menke and P. Maybeck, "Sensor/actuator failure detection in the vista F–16 by multiple model adaptive estimation," *IEEE Transactions on Aerospace and Electronic Systems*, vol. 31, pp. 1218–1229, October 1995.

[4] P. Eide and P. Maybeck, "An MMAE failure detection system for the F–16," *IEEE Transactions on Aerospace and Electronic Systems*, vol. 32, pp. 1125–1136, July 1996.

[5] Y. Zhang and X. Li, "Detection and diagnosis of sensor and actuator failures using IMM estimator," *IEEE Transactions on Aerospace and Electronic Systems*, vol. 34, pp. 1293–1313, October 1998.

[6] S. Dassanake, G. Balas, and J. Bokor, "Using unknown input observers to detect and isolate sensor faults in a turbofan engine," in *DASC 2000 – The 19th Digital Avionics Systems Conferences Proceedings*, vol. 2, pp. 6E5/1 – 6E5/7, IEEE, 7–13 October 2000.

[7] C. De Persis, R. De Santis, and A. Isidori, "Nonlinear actuator fault detection and isolation for a VTOL aircraft," in *Proceedings of the ACC 2001 American Control Conference*, vol. 6, pp. 4449–4454, IEEE, 25–27 June 2001.

[8] C. Belcastro, "Application of failure detection, identification, and accommodation methods for improved aircraft safety," in *Proceedings of*

the ACC 2001 American Control Conference, vol. 4, pp. 2623–2624, IEEE, 25–27 June 2001.

[9] B. Bacon, A. Ostroff, and S. Joshi, "Reconfigurable NDI controller using inertial sensor failure detection & isolation," *IEEE Transactions on Aerospace and Electronic Systems*, vol. 37, pp. 1373–1383, October 2001.

[10] C. Belcastro and B. Weinstein, "Distributed detection with data fusion for malfunction detection and isolation in fault tolerant flight control computers," in *Proceedings of the 2002 American Control Conference*, pp. 4224–4231, 8–10 May 2002.

[11] P. Samara, J. Sakellariou, G. Fouskitakis, and S. Fassois, "Detection of sensor abrupt faults in aircraft control systems," in *CCA 2003 – Proceedings of 2003 IEEE Conference on Control Applications*, vol. 2, pp. 1366–1371, IEEE, 23–25 June 2003.

[12] R. Isermann, "Supervision, fault detection and fault diagnosis methods: an introduction," *Control Engineering Practice*, vol. 5, no. 5, pp. 639–652, 1997.

[13] R. Mehra, C. Rago, and S. Seereeram, "Autonomous failure detection, identification and fault–tolerant estimation with aerospace applications," in *Proceedings of the 1998 IEEE Aerospace Conference*, vol. 1, pp. 133–138, IEEE, 21–28 March 1998.

[14] C. Hajiyev and F. Caliskan, "Fault detection in flight control systems via innovation sequence of Kalman filter," in *UKACC International Conference on Control 1998*, vol. 2, pp. 1528–1533, IEEE, 1–4 September 1998. (Conf. Publ. No. 455).

[15] J. Gertler, *Fault Detection and Diagnosis in Engineering Systems*. New York: Marcel Dekker, 1998.

[16] J. Chen and R. J. Patton, *Robust Model–Based Fault Diagnosis for Dynamic Systems*. Kluwer Academic Publishers, 1999.

[17] R. J. Patton, P. M. Frank, and R. N. Clark, eds., *Issues of Fault Diagnosis for Dynamic Systems*. London Limited: Springer–Verlag, 2000.

[18] S. Simani, C. Fantuzzi, and R. J. Patton, *Model-based fault diagnosis in dynamic systems using identification techniques.* Advances in Industrial Control, London, UK: Springer–Verlag, first ed., November 2002. ISBN 1852336854.

[19] S. Glavaski and M. Elgersma, "Active aircraft fault detection and isolation," in *AUTOTESTCON Proceedings, 2001 – IEEE Systems Readiness Technology Conference*, pp. 692–705, IEEE, 20–23 August 2001.

[20] IFAC, ed., *ACA 2004. 16^{th} IFAC Symposium on Automatic Control in Aerospace*, (St. Petersburg, Russia), IFAC, Elsevier, 14–18 June 2004.

[21] P. M. Frank, "Analytical and qualitative model–based fault diagnosis: a survey and some new results," *European Journal of Control*, vol. 2, no. 1, pp. 6–28, 1996.

[22] R. Isermann and P. Ballé, "Trends in the application of model-based fault detection and diagnosis of technical processes," *Control Engineering Practice*, vol. 5, no. 5, pp. 709–719, 1997.

[23] P. M. Frank, S. X. Ding, and B. Köpper-Seliger, "Current Developments in the Theory of FDI," in *SAFEPROCESS'00: Preprints of the IFAC Symposium on Fault Detection, Supervision and Safety for Technical Processes*, vol. 1, (Budapest, Hungary), pp. 16–27, 2000.

[24] M. Oosterom and R. Babuska, "Virtual sensor for fault detection and isolation in flight control systems – fuzzy modeling approach," in *Proceedings of the 39th IEEE Conference on Decision and Control*, vol. 3, pp. 2645–2650, IEEE, 12–15 December 2000.

[25] T. Curry, E. J. Collins, and M. Selekwa, "Robust fault detection using robust l_1 estimation and fuzzy logic," in *Proceedings of the ACC 2001 American Control Conference*, vol. 2, pp. 1753–1758, IEEE, 25–27 June 2001.

[26] T. Brotherton and T. Johnson, "Anomaly detection for advanced military aircraft using neural networks," in *IEEE Proceedings of the 2001 Aerospace Conference*, vol. 6, pp. 3113–3123, IEEE, March 2001.

[27] M. El-Ayadi, "Nonstochastic adaptive decision fusion in distributed–detection systems," *IEEE Transactions on Aerospace and Electronic Systems*, vol. 38, pp. 1158–1171, October 2002.

[28] J. Boskovic, L. Sai-Ming, and R. Mehra, "On–line failure detection and identification (fdi) and adaptive reconfigurable control (arc) in aerospace applications," in *Proceedings of the ACC 2001 American Control Conference*, vol. 4, pp. 2625–2626, IEEE, 25–27 June 2001.

[29] S. Mehra, R.and Seereeram, D. Bayard, and F. Hadaegh, "Adaptive Kalman filtering, failure detection and identification for spacecraft attitude estimation," in *Proceedings of the 4th IEEE CCA 1995 Conference on Control Applications*, pp. 176–181, IEEE, 28–28 September 1995.

[30] M. Bonfè, S. Simani, P. Castaldi, and W. Geri, "Residual generator computation for fault detection of a general aviation aircraft," in *ACA 2004. 16^{th} IFAC Symposium on Automatic Control in Aerospace*, (St. Petersburg, Russia), IFAC, 14–18 June 2003. (accepted).

[31] M. R. Napolitano, D. A. Windon, J. L. Casanova, and M. Innocenti, "Kalman Filters and Neural–Network Schemes for Sensor Validation in Flight Control Systems," *IEEE Transaction on Control System Technology*, vol. 6, no. 5, pp. 596–611, 1998.

[32] S. Simani, C. Fantuzzi, and S. Beghelli, "Diagnosis techniques for sensor faults of industrial processes," *IEEE Transactions on Control Systems Technology*, vol. 8, pp. 848–855, September 2000.

[33] F. Amato, C. Cosentino, M. Mattei, and G. Paviglianiti, "An Hybrid Direct/Functional Redundancy Scheme for the FDI of a small Commercial Aircraft," in *SAFEPROCESS'03 IFAC Symposium*, (Washington D.C.), 2003.

[34] M. Fink and D. Freeman, "Full-scale wind-tunnel investigation of static longitudinal and lateral characteristics of a light twin-engine airplane," Tech. Rep. TN D-4983, N.A.S.A., 1969.

[35] J. Koziol, "Simulation model for the Piper PA–30 light maneuverable aircraft in the final approach," Tech. Rep. DOT-TSC-FAA-71-11, N.A.S.A., 1971.

[36] J. Randle and M. Horton, "Low cost navigation using micro–machined technology," in *ITSC'97 – IEEE Conference on Intelligent Transportation System*, pp. 1064–1067, 9–12 November 1997.

[37] A. E. J. Bryson, *Control of Spacecraft and Aircraft*. UK: Princeton University, UK, 1994. ISBN 0-691-08782-2.

[38] ARINC, "Aeronautical Radio Inc.," in *MD. ARINC characteristic 706–4, Mark 5 subsonic air data system*, (Annapolis), 1998.

[39] R. P. Guidorzi, "Canonical Structures in the Identification," *Automatica*, vol. 11, pp. 361–374, 1975.

[40] T. Kailath, *Linear systems*. Englewood Cliffs, New Jersey 07632: Prentice Hall, 1980.

[41] E. Frisk, "Order of residual generators–bound and algorithms," in *SAFEPROCESS'2000: Proc. of IFAC Symposium on Fault Detection, Supervision and Safety for Technical Processes*, vol. 1, (Budapest, Hungary), pp. 599–604, 2000.

[42] E. Frisk and M. Nyberg, "A minimal polynomial basis solution to residual generation for fault diagnosis in linear systems," *Automatica*, vol. 37, no. 9, pp. 1417–1424, 2001.

[43] C. Houck, J. Joines, and M. Kay, "A Genetic Algorithm for Function Optimization: A Matlab Implementation," Tech. Rep. NCSU–IE TR 95–09, North Carolina State University, Raleigh, NC, USA, 1995. (available at `ftp://ftp.eos.ncsu.edu/pub/simul/GAOT`).